

Color Superconductivity in High Density Quark Matter

Stephen D.H. Hsu*

Department of Physics,

University of Oregon, Eugene OR 97403-5203

March, 2000

Abstract

We review recent progress on the phenomena of color superconductivity in high density quark matter. We begin with a brief overview of the unique aspects of physics near a Fermi surface and the implications for renormalization group (RG) techniques. We next discuss the qualitative differences between asymptotic densities, where the effective coupling constant can be made arbitrarily small, and intermediate densities where quark matter is still strongly coupled. It is in the latter regime where RG techniques are particularly useful, in that they yield a generic description of possible behaviors without relying on an expansion in the strong coupling constant. Finally, we discuss aspects of the QCD groundstate at asymptotic densities, which can be determined in a systematic weak coupling expansion.

Contribution to the Proceedings of the TMU-Yale Symposium on the Dynamics of Gauge Fields, December 13-15 1999, Tokyo, Japan.

*hsu@duende.uoregon.edu

1 Introduction

In this article I review recent progress on color superconductivity in high density QCD. It is remarkable how much more we know about QCD at high density compared to just two years ago, in 1998. The ultimate fate of baryonic matter at high density is a fundamental property of QCD, with implications for the astrophysics of neutron stars, as well as heavy ion collisions. More generally, we would like someday to understand the QCD phase diagram (figure (1)) in all its complexity as a function of temperature, chemical potential and quark masses.

While lattice studies have been fundamental in determining the behavior of QCD at high temperature, technical difficulties arise in the application of Monte Carlo techniques once a chemical potential is introduced (essentially, the measure of integration is no longer positive definite, due to complex eigenvalues of the Dirac operator). The progress I describe does not rely on brute force techniques, but rather on physical insights associated with the presence of a Fermi surface. The special properties of physics near a Fermi surface are discussed in section 2. Remarkably, rigorous statements can be made in the limit of infinite density.

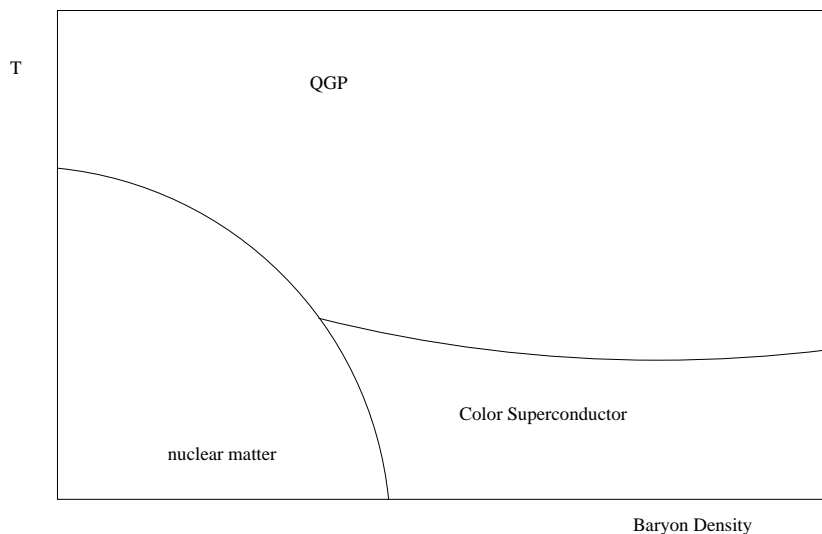


Figure 1: The QCD Phase Diagram as a function of temperature and density.

There are two qualitatively different regimes to be addressed. The regime most likely to be realized in nature (i.e. in the cores of neutron stars or in heavy ion collisions) is that of intermediate density, where the average distance between quarks is still of order a Fermi and the gluons exchanged are rather soft. This regime is strongly coupled, and while we can make qualitative statements about the nature of the ground state using renormalization group techniques, we cannot perform quantitative calculations. The intermediate density case is discussed in section 2.

At extremely high densities the effective coupling α_s is small, leading to a weakly coupled liquid of quarks. The only low energy excitations in this liquid are quasi-particles and quasi-holes representing fluctuations near the Fermi surface. There are rather general arguments (see below) which suggest that any attractive interaction, no matter how small, can lead to Cooper pairing in the presence of a Fermi surface. In the case of QCD, this attractive interaction is provided by gluon exchange in the $\bar{3}$ channel. Thus, we expect to find condensation of Cooper pairs of quarks in the high density limit.

Actually, even in the high density limit, there are some subtleties which make the problem less than straightforward. Most importantly, although the effective coupling is weak, the exchange of magnetic gluons leads to a long range interaction due to the absence of a magnetic screening mass. Quarks carry electric, rather than magnetic, color charge, and hence are better at screening the timelike component (A_0) of the gluon field than the spacelike (A_i). It is only non-perturbative effects which can screen color-magnetic fluctuations, and these are nearly absent at weak coupling. An understanding of dynamic screening due to Landau damping is necessary to control the high density calculations. These issues are discussed in section 4.

The order parameter for color superconductivity is

$$\langle \psi^T C \Gamma \psi \rangle \quad . \quad (1)$$

where C is the charge conjugation operator and Γ is a matrix in color, flavor and Dirac space. As we will see below, determining the precise form of Γ requires some work; it is particularly complicated in the case of three flavors. However, as we will discuss in section 5, in the weak coupling limit the true groundstate can be determined in a controlled approximation. Here we will simply note that single gluon exchange between two quark quasiparticles can be decomposed into an attractive $\bar{3}$ channel and a repulsive 6 channel. Thus, at the most naive level we expect an anti-triplet condensate, which breaks $SU(3) \rightarrow SU(2)$. The main effect of this condensate is that it leads to the Higgs phenomena for at least some subset of the gluons, or equivalently to the Meissner effect and screening of some subset of the color magnetic fields. The phenomenological implications of color superconductivity are still not well understood and will be the subject of investigation for some time to come.

Let me close this introduction with a historical note. The idea that quark matter might be a color superconductor is quite old [1, 2, 3]. The original insight was based on the existence of the attractive $\bar{3}$ channel and an analogy with ordinary superconductors. Recent interest in the problem was rekindled by the work of two groups that considered diquark condensation due to instanton-mediated interactions [4], predicting gaps as large as ~ 100 MeV. These calculations, while uncontrolled, are quite suggestive, and led to the recent progress on the subject. It is often claimed that early investigations predicted tiny gaps, at most of order a

few MeV. While this may have been the consensus among the few theorists who had actually worked on the problem, it is actually an unfair characterization of Bailin and Love's results [3]. A value of the strong coupling large enough to justify the instanton liquid picture of [4] also yields a large gap when substituted in Bailin and Love's results. After all, instantons are suppressed by an exponential factor $\exp(-2\pi/\alpha_s)$. Bailin and Love merely suffered from the good taste not to extrapolate their results to large values of α_s !

2 Physics Near a Fermi Surface and the Renormalization Group

Important simplifications arise in the study of cold, dense matter due to the existence of a Fermi surface, which in relativistic systems is likely to be rotationally invariant. The energy of a low-energy excitation (a quasi-particle or -hole) is then independent of the orientation of its momentum \vec{p} , and only depends on $p - \mu$, where $p = |\vec{p}|$ and μ is the chemical potential or Fermi energy. (Here, for simplicity, we will always work with massless quarks.) This leads to a kind of dimensional reduction, so that physics near a Fermi surface is effectively 1+1 dimensional. In particular, arbitrarily weak interactions can lead to non-perturbative phenomena like pair formation.

The renormalization group approach [5] is particularly useful here – we integrate out the modes far from the Fermi surface, leaving only the low-energy quasi-particle and -hole states that are involved in the interesting physics. These excitations might in principle be related to the original quarks in a complicated way, but on quite general grounds must be described by an effective action of the form

$$S_{eff} = \int dt d^3p \psi^\dagger (i\partial_t - (\epsilon(p) - \epsilon_F)) \psi + S_{int}, \quad (2)$$

where S_{int} contains higher dimensional, local quasi-particle operators. Strictly speaking, this form of the effective action is only valid for models in which the original interactions were local (short ranged). While appropriate for QCD at intermediate densities [6, 7], where non-perturbative effects are expected to generate screening of magnetic gluons, it must be modified at weak coupling where magnetic fluctuations are long ranged [10, 11]. However, it is the only technique I know of from which we can obtain robust information about the strongly coupled region of the phase diagram. Below I review the results of this analysis, and defer a discussion of the weak coupling phase until the following section.

It can be shown [6, 7] using simple classical scaling arguments that all interactions are irrelevant except for the Cooper pairing interaction (scattering of quasi-particles at opposite

sides of the Fermi surface: $\vec{p}_1 \simeq -\vec{p}_2$) and strictly colinear scattering: $\vec{p}_1 \simeq \vec{p}_2$, which can lead to the Overhauser effect (chiral waves) at large- N_c [8]. Both of these interactions are classically marginal, so quantum corrections determine their evolution. Here we restrict ourselves to local Cooper pairing operators which are invariant under the full $SU(3)_L \times SU(3)_R \times U(1)_A$ chiral symmetry:

$$\begin{aligned} O_{LL}^0 &= (\bar{\psi}_L \gamma_0 \psi_L)^2, & O_{LR}^0 &= (\bar{\psi}_L \gamma_0 \psi_L)(\bar{\psi}_R \gamma_0 \psi_R) \\ O_{LL}^i &= (\bar{\psi}_L \gamma_i \psi_L)^2, & O_{LR}^i &= (\bar{\psi}_L \vec{\gamma} \psi_L)(\bar{\psi}_R \vec{\gamma} \psi_R). \end{aligned} \quad (3)$$

These come in both color symmetric ($\bar{3}$) and antisymmetric (sextet) combinations. More general operators with different flavor or Dirac structures can be reduced to linear combinations of the basic ones (3), using parity and Fierz rearrangements. This analysis can be extended to operators (such as those induced by instantons) that break the anomalous $U(1)_A$ symmetry [6, 7], yielding a very robust characterization of QCD even at intermediate densities and strong coupling. We will not discuss the details of this more general analysis here, but the results (given reasonable assumptions about the signs and magnitudes of the interactions) are qualitatively similar

The RG evolution of the operators in (3) is determined by quark-quark scattering near the Fermi surface. A bubble graph with four-quark vertices Γ_1 and Γ_2 and external quark lines satisfying the Cooper pairing kinematics yields

$$G_1 G_2 I (\Gamma_1)_{i'i} (\Gamma_1)_{k'k} \left[-(\gamma_0)_{ij} (\gamma_0)_{kl} + \frac{1}{3} (\vec{\gamma})_{ij} (\vec{\gamma})_{kl} \right] (\Gamma_2)_{j'j} (\Gamma_2)_{l'l} \quad (4)$$

Here $I = \frac{i}{8\pi^2} \mu^2 \log(\Lambda_{IR}/\Lambda_{UV})$, where $[\Lambda_{IR}, \Lambda_{UV}]$ are the upper and lower cutoffs of the momentum shell integrated out. We define the density of states on the Fermi surface to be $N = \mu^2/(2\pi^2)$ (in weak coupling) and $t \equiv \log(\Lambda_{IR}/\Lambda_{UV})$. The RG flow does not mix LL and LR operators, nor different color channels. We obtain the following RG equations

$$\frac{d(G_0^{LL} + G_i^{LL})}{dt} = -\frac{N}{3} (G_0^{LL} + G_i^{LL})^2, \quad (5)$$

$$\frac{d(G_0^{LL} - 3G_i^{LL})}{dt} = -N (G_0^{LL} - 3G_i^{LL})^2, \quad (6)$$

$$\frac{d(G_0^{LR} + 3G_i^{LR})}{dt} = 0, \quad (7)$$

$$\frac{d(G_0^{LR} - G_i^{LR})}{dt} = -\frac{2N}{3} (G_0^{LR} - G_i^{LR})^2. \quad (8)$$

The linear combination $G_* = G_0^{LL} + G_i^{LL}$ reaches its Landau pole first, governed by the equation

$$G_*(t) = \frac{1}{1 + (N/3)G_*(0)t} \quad (9)$$

In general, interactions which are attractive at the matching scale, $G_*(0) > 0$, will grow during the evolution, and reach a Landau pole at the scale $t_* = -3/(NG_*(0))$. The corresponding energy scale is

$$\Lambda_{IR} = \Lambda_{UV} \exp\left(-\frac{3}{NG_*(0)}\right), \quad (10)$$

which agrees with the usual BCS result. Repulsive interactions, corresponding to negative initial values of the coupling, become weaker near the Fermi surface.

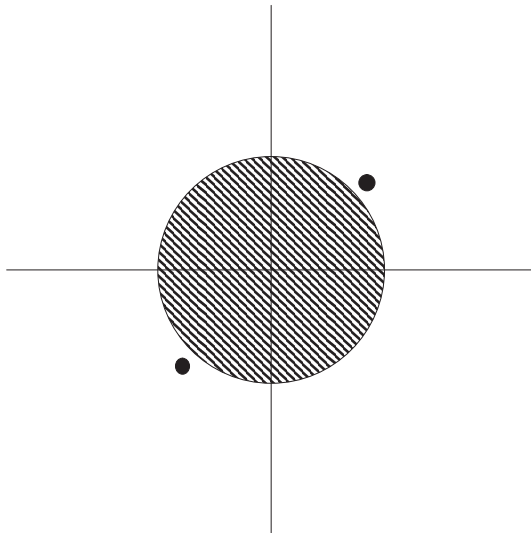


Figure 2: Excitations on opposite sides of the Fermi surface.

3 High Density Limit

In the high density limit the typical momentum transfer between quarks is large, and therefore the effective coupling is small. The properties of this phase can be deduced in a systematic, weak coupling expansion. However, there is one technical problem that must be solved having to do with soft magnetic gluons. In the renormalization of the Cooper pairing interaction there is a region of phase space where the incoming quarks are only slightly deflected by the gluon exchange. This leads to an IR divergence unless arbitrarily soft gluons are screened in some way. While gluons acquire a perturbative electric mass at high density, it can be shown that to all orders in perturbation theory no magnetic mass is generated [9]. The only hope is that Landau damping – a form of dynamic screening affecting the spacelike gluons – is enough to control this IR problem. That this is so was first pointed out by Son [10], who went on to deduce the following behavior for the diquark gap at weak coupling

$$\Delta \sim \mu g^{-5} \exp\left(-\frac{3\pi^2}{\sqrt{2}g}\right) . \quad (11)$$

This result has since been confirmed by RG methods [11] as well as Schwinger-Dyson techniques [12]. In this section I discuss some of the details of these calculations, concentrating on the the RG approach.

The magnetic gluon propagator, including vacuum polarization effects from virtual quarks, [9] has the form ($q_0 \ll q$)

$$D_{\mu\nu}^T(q_0, q) = \frac{P_{\mu\nu}^T}{q^2 + i\frac{\pi}{2}m_D^2 \frac{|q_0|}{q}} \quad . \quad (12)$$

Strictly speaking $D_{\mu\nu}^T$ is gauge dependent, but in our leading order calculations the propagator always appears contracted with gamma matrices next to nearly on-shell external quark lines. Thus the gauge dependent parts are higher order in g due to the equations of motion. The effect of Landau damping is to cut off the small- q divergence in (12) at $q \sim q_0^{1/3} m_D^{2/3}$, where $m_D^2 = N_f \frac{g^2 \mu^2}{2\pi^2}$ is the Debye screening mass. A common feature of both the Schwinger-Dyson and RG calculations in the weak coupling region is loop integrals dominated by energy transfers of order $q_0 \sim \Delta$, and hence momentum transfers of order $q_* \sim \Delta^{1/3} m_D^{2/3}$. q_* can be made as large as desired by going to high density.

The main technical problem in the RG approach is long range magnetic interactions, or equivalently the presence of soft gluons. At no point can the theory be completely described by quarks with purely local interactions as in (2). The effective Lagrangian contains both quark and gluon excitations (with energies below the cutoff Λ) and local interactions resulting from integration of higher energy shells. This modifies the form of the RG equations obtained [11], so that equations (5) and (6) become

$$\frac{d(G_0^{LL} + G_i^{LL})}{dt} = -\frac{N}{3}(G_0^{LL} + G_i^{LL})^2 - \frac{g^2}{9\mu^2} \quad , \quad (13)$$

$$\frac{d(G_0^{LL} - 3G_i^{LL})}{dt} = -N(G_0^{LL} - 3G_i^{LL})^2 + \frac{g^2}{27\mu^2} \quad . \quad (14)$$

The solution of these RG equations leads to a Landau pole in the dominant $\bar{3}$, LL and RR channels given by (11). It is worth commenting on the angular momentum of the condensate. The RG equations can be derived for general values of angular momentum l . Naively interpreted, the results suggest that condensates might occur in higher l channels, leading to the breaking of O(3) rotational invariance. A more detailed gap equation analysis [11] shows that this is not the case: a large s-wave gap suppresses the formation of p-wave and higher l gaps. The literature is somewhat confused on this important issue. The papers in [13] address the issue of rotational invariance and do not agree on the size of higher l gaps. However, neither paper addresses the interplay of s-wave and higher l gaps, which is studied in [11].

4 The QCD Groundstate at High Density

In this section I describe the vacuum energy analysis necessary to determine the groundstate of QCD at high density [14]. Neither the RG nor Schwinger-Dyson analyses are sufficient to specify the actual groundstate. Strictly speaking, the former only reveals the energy scale and quantum numbers of the pairing instability, while the latter only identifies extrema of the vacuum energy. As we shall see, there are additional subtleties which can only be resolved by consideration of energetics.

First, let us consider the case of 2 massless flavors. Because the condensate occurs between pairs of either left (LL) or right (RR) handed quarks in the $J=L=S=0$ channel [11], and the $\bar{3}$ color channel is antisymmetric, the quarks must pair in the isospin singlet ($ud - du$) flavor channel. However, even in this case there is a subtlety, as the relative color orientations of the LL and RR condensates are not determined by the usual leading order analysis. A misalignment of these condensates violates parity, and further breaks the gauge group beyond $SU(3)_c \rightarrow SU(2)_c$. An analysis of the Meissner effect is necessary to determine the relative orientation [14], and the effect is higher order in g . There are thus a number of unstable configurations of only slightly higher energy with different color-flavor orientations (and hence different symmetry breaking patterns), leading to the possibility of disorienting the diquark condensate (see figure (3)).

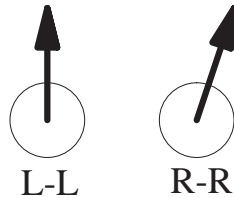


Figure 3: Color disorientation of LL and RR condensates.

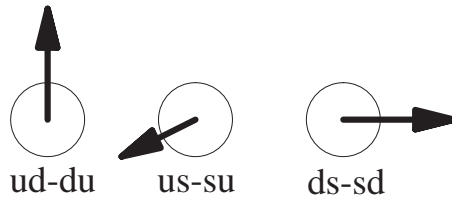


Figure 4: CFL condensation: each flavor channel chooses an orthogonal color orientation.

The generalization to three flavors is far from straightforward. Again, one can show that the condensate must occur in the $J=L=S=0$ and color $\bar{3}$ channel. (The sextet condensate is suppressed in the weak coupling limit [14] and I do not discuss it here.) The Pauli principle

then requires that the flavor structure again be antisymmetric $\sim (q_i q_j - q_j q_i)$, for quarks of flavor i, j . Thus, one can have combinations of condensates which are in the $\bar{3}$ of both color and flavor $SU(3)_L$ or $SU(3)_R$. Due to the chirality preserving nature of perturbative gluon exchange, there is no mixing of LL and RR condensates, which form independently. One can immediately see that there are a number of possibilities. For example, the condensates for the three flavors and both chiralities might all align in color space, leading to an $SU(3)_c \rightarrow SU(2)_c$ breaking pattern. A more complicated condensate has been proposed [15, 16] called Color Flavor Locking (CFL), in which the $\bar{3}$ color orientations are “locked” to the $\bar{3}$ flavor orientation. In figure (4) we give a simple picture of CFL condensation.

To determine the nature of the energy surface governing the various color-flavor orientations of the condensate, we can begin by characterizing the color-flavor configuration space of condensates. We consider the ansatz

$$\Delta_{ij}^{ab L,R} = A_k^{c L,R} \epsilon^{abc} \epsilon_{ijk} \quad , \quad (15)$$

where a,b are color and i,j flavor indices. L and R denote pairing between pairs of left and right handed quarks, respectively. Under color and flavor A transforms as

$$A^L \rightarrow U_c A^L V^L \quad , \quad (16)$$

where U_c is an element of $SU(3)_c$ and V^L of $SU(3)_L$. A similar equation holds for A^R . It is always possible to diagonalize A^L by appropriate choice of U_c and V^L :

$$A^L = \begin{pmatrix} a & 0 & 0 \\ 0 & b & 0 \\ 0 & 0 & c \end{pmatrix} \quad . \quad (17)$$

Generically, there does not exist a V^R which diagonalizes A^R in this basis. In the CFL case, where the diagonalized A^L is proportional to the identity, $a = b = c$, it is easy to show that one can choose V^R such that $A^R = \pm A^L$. These two configurations are related by a $U(1)_A$ rotation (see section 3). Hence, they are degenerate in the high density limit where gluon exchange dominates. Instanton effects, important at intermediate density, favor $A^R = A^L$. Note that parity, if unbroken, requires $A^L = A^R$, and hence implies simultaneous diagonalizability.

In [14] we considered the potential vacua parametrized by a,b,c. First, we use the Dyson-Schwinger (gap) equation to determine which of these configurations are energy extrema. Next, we computed the energies of the extrema to determine the true groundstate. A similar analysis has been carried out by Schäfer and Wilczek [16] in the approximation where gluon interactions are replaced by local four fermion interactions. They concluded that the CFL

vacuum had the lowest energy. In our analysis, which I summarize below, we included the gluons in the analysis, introducing long range color-magnetic fluctuations (controlled by Landau damping) and Meissner screening into the gap equation and vacuum energy calculations.

At asymptotically high densities (weak coupling) the diagrams (a)-(c) in figure (5) give the leading approximation to the effective action. Note that in these diagrams the quark propagators include the diquark condensate (see (20) below), and the gluon propagators include Landau damping, but *not* the Meissner effect. The latter arises from the condensate-dependence of quark loops in diagrams (c) and (d). The resulting gap equation (figure (6)), with condensate shown explicitly at lowest order in Δ) is given by

$$S^{-1}(q) - S_0^{-1}(q) = ig^2 \int \frac{d^4k}{(2\pi)^4} \Gamma_\mu^A S(k) \Gamma_\nu^B D_{AB}^{\mu\nu}(k-q), \quad (18)$$

where

$$\Gamma_\mu^A = \begin{pmatrix} \gamma_\mu T^A & 0 \\ 0 & C(\gamma_\mu T^A)^T C^{-1} \end{pmatrix}. \quad (19)$$

$D_{AB}^{\mu\nu}$ is the gluon propagator, including the effects of Landau damping and Debye screening (we assume Feynman gauge throughout).

We will restrict the color group structure in the gap equation to the attractive anti-symmetric $\bar{3}$ channel, which projects out the anti-symmetric part of $S(k)$ in color space in the gap equation. Here S is the fermion propagator for the spinor (ψ_a^i, ψ_a^{iC}) with i a flavor index and a a color index.

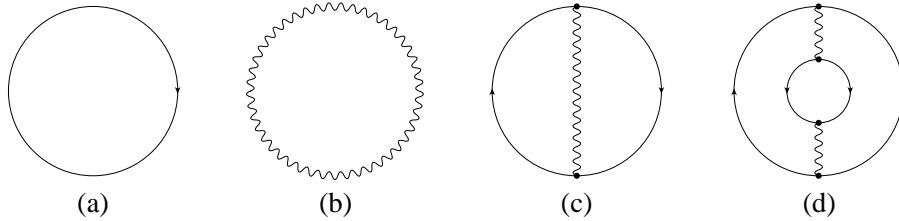


Figure 5: Vacuum energy diagrams.

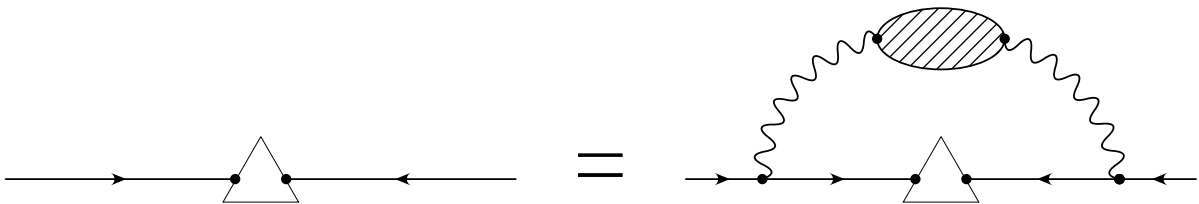


Figure 6: Schwinger-Dyson equations.

For the three flavor case S can be written explicitly as an 18×18 matrix in color flavor space. The inverse propagator may be written

$$S^{-1}(q) = \begin{pmatrix} \not{q} + \not{\mu} & \gamma_0 \Delta^\dagger \gamma_0 \\ \Delta & \not{q} - \not{\mu} \end{pmatrix} \quad (20)$$

where $\not{\mu} = \mu \gamma_0$. Δ is a 9×9 matrix which for the ansatz (17) takes the form

$$\Delta = \begin{pmatrix} 0 & 0 & 0 & 0 & c & 0 & 0 & 0 & b \\ 0 & 0 & 0 & -c & 0 & 0 & 0 & 0 & 0 \\ 0 & 0 & 0 & 0 & 0 & 0 & -b & 0 & 0 \\ 0 & -c & 0 & 0 & 0 & 0 & 0 & 0 & 0 \\ c & 0 & 0 & 0 & 0 & 0 & 0 & 0 & a \\ 0 & 0 & 0 & 0 & 0 & 0 & 0 & -a & 0 \\ 0 & 0 & -b & 0 & 0 & 0 & 0 & 0 & 0 \\ 0 & 0 & 0 & 0 & 0 & -a & 0 & 0 & 0 \\ b & 0 & 0 & 0 & a & 0 & 0 & 0 & 0 \end{pmatrix} \quad (21)$$

Because we are dealing with a diquark condensate the non-trivial part of the gap equation involves the lower left 9×9 block. We will refer to this sub-block of the propagator S as S_{21} .

For a particular ansatz Δ to be a solution to the gap equation we require that the color antisymmetric part of $T^A S_{21}(k) T^A$ (corresponding to the $\bar{3}$ channel) be proportional in color-flavor space to the off-diagonal 21 submatrix of $S^{-1}(q) - S_0^{-1}(q)$, or $\Delta(q)$, which appears on the LHS of the gap equation (see [14] for more discussion of this point).

The propagator may be found by inverting the sparse matrix in (20) using Mathematica. Only three ansätze satisfy our condition: $a = b = c$; $a = b, c = 0$; $b = c = 0$. We refer to these solutions as (111) (color-flavor locking), (110) ($3 \rightarrow 0$ breaking) and (100) ($3 \rightarrow 2$ breaking) respectively. For these ansätze the color antisymmetric part of $T^A S_{21}(k) T^A$ has the form of a constant multiplying the matrix form (21) with a, b, c set to 0 or 1 as is appropriate for the ansatz. After contour integration over l , we find the following gap kernels

$$\begin{aligned} (111) & : \frac{2}{3} \frac{\Delta}{\sqrt{k_0^2 + \Delta^2}} + \frac{1}{3} \frac{\Delta}{\sqrt{k_0^2 + 4\Delta^2}} \\ (110) & : \frac{\Delta}{2\sqrt{k_0^2 + \Delta^2}} + \frac{\Delta}{2\sqrt{k_0^2 + 2\Delta^2}} \\ (100) & : \frac{\Delta}{\sqrt{k_0^2 + \Delta^2}} \end{aligned} \quad (22)$$

These kernels are to be substituted in the following gap equation, which we obtain under the approximation $q_0 \ll |\vec{q}|$. (We also neglected the anti-particle contributions, which are suppressed by powers of $1/\mu$.)

$$\Delta(p_0) = \frac{g^2}{12\pi^2} \int dq_0 \int d\cos\theta \left(\frac{\frac{3}{2} - \frac{1}{2}\cos\theta}{1 - \cos\theta + (G + (p_0 - q_0)^2)/(2\mu^2)} + \frac{\frac{1}{2} + \frac{1}{2}\cos\theta}{1 - \cos\theta + (F + (p_0 - q_0)^2)/(2\mu^2)} \right) K(q_0), \quad (23)$$

where F and G represent the medium effects on the electric and magnetic gluons, and $K(q_0)$ is one of the gap kernels from (22). The Meissner effect makes an additional contribution to G beyond that of Landau damping. In [14] we evaluated the gluon vacuum polarization $P_{\mu\nu}(q_0, q)$ in the presence of a diquark condensate. (A more detailed computation of the Meissner effect is given by Rischke [17], with similar results.) The additional Meissner screening is given by $\delta G \equiv \frac{1}{2}\mathcal{P}_{ij}^T P_{ij}$, where $\mathcal{P}_{ij}^T = (\delta_{ij} - \hat{q}_i \hat{q}_j)$ is the transverse projection operator. At low momenta, $q_0, q \sim \Delta$, $\delta G(q_0, q)$ is of order the Debye mass $m_D \sim g\mu$, while at larger energy or momenta the effect is suppressed by a power of $\frac{\Delta}{q_0}$ or $\frac{\Delta}{q}$. We limited ourselves to an estimate of the size of the Meissner effect on the gap solutions. To this end, we used the following approximation for δG :

$$\delta G(q_0, q) \simeq m_D^2 \frac{\Delta_0}{\sqrt{q^2 + q_0^2 + \Delta_0^2}}, \quad (24)$$

where Δ_0 is the maximum value of the function $\Delta(k_0, k)$. Note we did not introduce any color structure in δG ; all gluons experience the same magnetic screening. While this is a crude approximation, it gives the rough size of the Meissner effect on Δ .

We solved the gap equations for all three gap kernels using this form of the Meissner effect, and the results are shown in figure (7) for the case of $\mu = 400$ MeV. The effect is to decrease the size of the condensate but it is a small perturbation on the solutions obtained without the Meissner effect.

To determine which of the above gaps is the true minimum energy state we must calculate the vacuum energy, which receives contributions from vacuum to vacuum loops of both quarks and gluons (figure 1). We start with the CJT effective potential [18], which upon extremization wrt appropriate propagators and vertices leads to the Schwinger-Dyson equations. The fermion equation is the gap equation given above, while the gluon equation reproduces Landau damping. We wish to compare energies corresponding to our three solutions to determine which one is the true vacuum (the difference in energies V will be gauge invariant, whereas actual values are not). It is easy to show that the value of the effective potential evaluated on the gap solution is given by:

$$V = -i \int \frac{d^4 p}{(2\pi)^4} \text{tr} \ln S(p) / S_0(p). \quad (25)$$

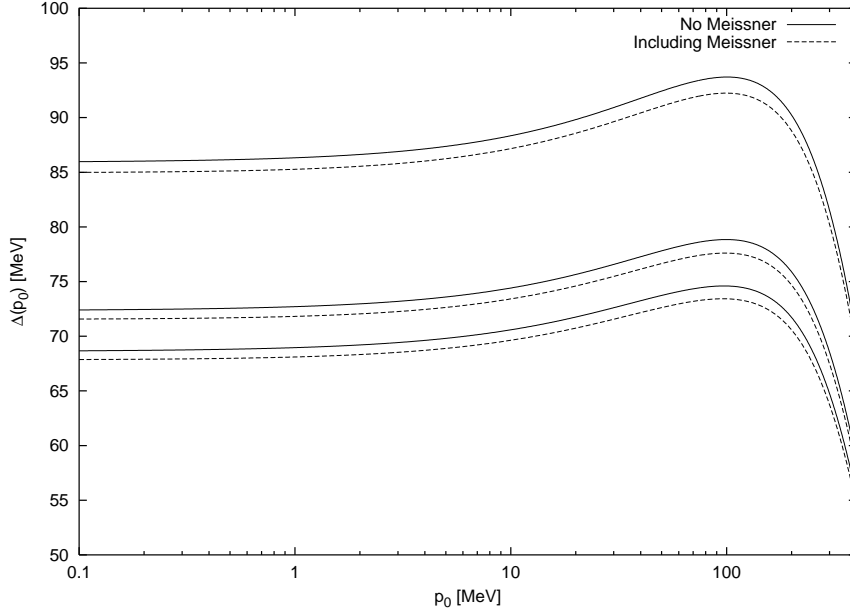


Figure 7: Gap solutions for $\mu = 400$ MeV, with and without Meissner effect.

Diagrammatically, this is equivalent to the graph of figure 1(a) when evaluated on the gap solution.

The fermion loops are most easily calculated by going to a basis where $S_0 S^{-1}$ is diagonal in color-flavor space. Note that the gap matrix Δ has non-trivial Dirac structure that must be accounted for [19]: $\Delta = \Delta_1 \gamma_5 P_+ + \Delta_2 \gamma_5 P_-$, where P_{\pm} are particle and anti-particle projectors. Our analysis has been restricted to the particle gap function Δ_1 . The anti-particle gap function Δ_2 has its support near $k_0 \sim 2\mu$, and its contribution to the vacuum energy is suppressed. There are 18 eigenvalues, which occur in 9 pairs. The product of each pair is of the form

$$- \left(1 + a \frac{\Delta^2(k_0, k)}{k_0^2 + (|\vec{k}| - \mu)^2} \right), \quad (26)$$

where a is an integer. For our three cases we obtain the following sets of eigenvalues:

$$\begin{aligned} (111) &\rightarrow 8 \times \{a = 1\}, 1 \times \{a = 4\} \\ (110) &\rightarrow 4 \times \{a = 1\}, 2 \times \{a = 2\} \\ (100) &\rightarrow 4 \times \{a = 1\} \end{aligned} \quad (27)$$

The binding energy is of order

$$E_q \sim - \int d^3k dk_0 \ln \left[1 + a \frac{\Delta^2(k_0, k)}{k_0^2 + (k - \mu)^2} \right] \quad (28)$$

$$\sim -a \mu^2 \Delta_0^2 , \quad (29)$$

where Δ_0 is the maximum value of the gap function $\Delta(k_0, k)$, which has rather broad support in both energy and momentum space away from the Fermi surface. A more precise answer than (28) requires numerical evaluation, but it is clear that the result scales with a and has only a weak (logarithmic) dependence on the variations in the shape of $\Delta(k_0, k)$. Substituting our numerical results for the gaps in the three cases, it is easy to establish that

$$E(111) < E(110) < E(100) . \quad (30)$$

We find that the CFL vacua remains the lowest energy state, at least at asymptotically high densities where the calculation is reliable. The Meissner effect is a small correction to the vacuum energy at asymptotic densities. Configurations which satisfy the gap equations but are not the global minimum of energy are presumably saddlepoints, since they are continuously connected to the CFL vacuum via color and flavor rotations.

5 Conclusions

In this contribution I have tried to summarize some important progress of the last two years on the theory of cold, dense quark matter. Due to space limitations, I was not able to discuss a number of important issues, such as the low energy effective Lagrangian, continuity of hadronic and quark phases and more phenomenological studies. I list some of the important papers in [20].

I thank my collaborators N. Evans, J. Hormuzdiar and M. Schwetz and my colleagues D. Hong, R. Pisarski, K. Rajagopal, M. Rho, D. Rischke and T. Schäfer for contributing to my understanding of this subject. My research was supported under DOE contract DE-FG06-85ER40224 and by a JSPS visiting fellowship.

References

- [1] S.C. Frautschi, *Proceedings of the Workshop on Hadronic Matter at Extreme Energy Density*, N. Cabibbo Editor, Erice, Italy (1978)
- [2] F. Barrois, Nucl. Phys. B129 (1977) 390.
- [3] D. Bailin and A. Love, Phys. Rep. 107, 325 (1984).

- [4] M. Alford, K. Rajagopal, and F. Wilczek, Phys. Lett. B422, 247 (1998); R. Rapp, T. Schäfer, E.V. Shuryak, and M. Velkovsky, Phys. Rev. Lett. 81, 53 (1998); hep-ph/9904353;
- [5] R. Shankar, Rev. Mod. Phys. 66, 129 (1995); J. Polchinski, hep-th/9210046.
- [6] N. Evans, S.D.H. Hsu, and M. Schwetz, Nucl. Phys. B551, 275 (1999); Phys. Lett. B449 281, (1999).
- [7] T. Schäfer and F. Wilczek, Phys. Lett. B450, 325 (1999).
- [8] D. V. Deryagin, D. Yu. Grigoriev, and V. A. Rubakov, Int. J. Mod. Phys. A7, 659 (1992); E. Shuster and D. T. Son, preprint, hep-ph/9905448; B.-Y. Park, M. Rho, A. Wirzba, and I. Zahed, preprint, hep-ph/9910347.
- [9] M. Le Bellac, *Thermal Field Theory* (Cambridge, Cambridge University Press, 1996).
- [10] D.T. Son, Phys. Rev. D 59, 094019 (1999).
- [11] S.D.H. Hsu and M. Schwetz, hep-ph/9908310 (to appear in Nucl.Phys.B).
- [12] T. Schäfer and F. Wilczek, preprint, hep-ph/9906512; R. D. Pisarski, D. H. Rischke, preprint, nucl-th/9907041; D. K. Hong, V. A. Miransky, I. A. Shovkovy, and L. C. R. Wijewardhana, preprint, hep-ph/9906478; W. E. Brown, J. T. Liu, and H. Ren, preprint, hep-ph/9908310.
- [13] R.D. Pisarski and D.H. Rischke, nucl-th/9910056; W. E. Brown, J. T. Liu, and H. Ren, hep-ph/9912409.
- [14] N. Evans, J. Hormuzdiar, S.D.H. Hsu, and M. Schwetz, hep-ph/9910313.
- [15] M. Alford, K. Rajagopal, and F. Wilczek, Nucl. Phys. B537, 443 (1999). M. Alford, J. Berges and K. Rajagopal, hep-ph/9903502.
- [16] T. Schäfer and F. Wilczek, Phys. Rev. Lett. 82, 3956 (1999); hep-ph/9903503.
- [17] D.H. Rischke, nucl-th/0001040.
- [18] J.M. Cornwall, R. Jackiw and E. Tomboulis, PRD10, 2428 (1974).
- [19] R.D. Pisarski and D.H. Rischke, Phys. Rev. D 60, 094013 (1999).

- [20] R.D. Pisarski and D.H. Rischke, Phys. Rev. Lett. 83, 37 (1999); J. Berges and K. Rajagopal, Nucl. Phys. B538, 215 (1999); G.W. Carter and D. Diakonov, Phys. Rev. D 60, 016004 (1999); K. Langfeld and M. Rho, hep-ph/9811227; M. Alford, J. Berges, and K. Rajagopal, hep-ph/9903502; D.K. Hong, hep-ph/9812510, hep-ph/9905523; D.K. Hong, M. Rho, and I. Zahed, hep-ph/9906551; R.D. Pisarski and D.H. Rischke, nucl-th/9906050; R. Casalbuoni and R. Gatto, hep-ph/9908227; hep-ph/9909419; D.T. Son and M.A. Stephanov, hep-ph/9910491; B.Y. Park, M. Rho, A. Wirzbad, and I. Zahed, SUNYSB-preprint.